



Xestosaprol D and E from the Indonesian marine sponge *Xestospongia* sp.

Natalie Millán-Aguíñaga^{a,b}, Irma E. Soria-Mercado^b, Philip Williams^{a,*}

^a Department of Chemistry, University of Hawaii at Manoa, Honolulu, Hawaii, 96822, United States

^b Facultad de Ciencias Marinas, UABC. Ensenada, Baja California, México, 22800, United States

ARTICLE INFO

Article history:

Received 11 November 2009

Revised 26 November 2009

Accepted 27 November 2009

Available online 3 December 2009

ABSTRACT

Chemical investigation of an extract of the marine sponge *Xestospongia* yielded a suite of pentacyclic compounds, including two new xestosaprol derivatives. Xestosaprol D (**1**) and E (**2**) are regioisomers, whose structures were defined through analysis of spectroscopic data.

© 2009 Elsevier Ltd. All rights reserved.

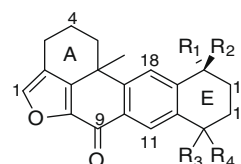
Indo-Pacific marine sponges of the genera *Xestospongia* and *Haliclona* produce polyketide quinones and hydroquinones with varying degrees of oxidation and unsaturation, exemplified by halenaquinone and xestoquinone.¹ A diverse array of activities have been attributed to these compounds including antibiotic,² antifungal,³ cardiotoxic,⁴ and cytotoxic⁵ activities. Specific cellular targets have also been identified in a few instances to include protein tyrosine kinases,⁶ topoisomerases,⁷ and myosin Ca²⁺ ATPase.⁸

In our continuing search for new bioactive substances from marine sources, we recently identified an extract derived from a *Xestospongia* sp. collected near Turtle Bay, Sangalaki, Indonesia, which significantly inhibited pathogenic multiple-resistant *Staphylococcus aureus* and weakly inhibited the aspartic protease BACE1. In this report, we describe the structural elucidation and biological activity of two new pentacyclic derivatives isolated from this extract, in addition to the biological testing of several related structures.

Xestosaprol D (**1**, Fig. 1) was isolated as an optically active yellow solid ($[\alpha]_D^{25}$ 18.8 (c 0.1, MeOH)) by repeated C₈ chromatography of the ethyl acetate extract. Vibrational bands in the IR spectrum at 3398 (br) and 1669 cm⁻¹ indicated the presence of hydroxyl and carbonyl functional groups. Based on the reduced strength of the latter vibration, the carbonyl was conjugated to the chromophore responsible for the 255 nm absorption maximum in the UV spectrum. A pseudomolecular isotope peak at m/z 323.1291 [M+H]⁺, obtained based on HR-ESI-TOFMS data, defined the molecular formula of **1** as C₂₀H₁₈O₄ (12 degrees of unsaturation). Analysis of the ¹³C NMR spectrum supported this formula, accounting for 10 quaternary carbons, 4 methines, 5 methylenes, and 1 methyl carbon (C₂₀H₁₇). On the basis of carbon chemical shift arguments, **1** contained one methyl group (δ_C 32.4), two carbonyl equivalents (δ_C 172.1 and 197.5), and 10 other sp² hybridized carbons. These

twelve carbons, accounting for seven double-bond equivalents, indicated that **1** was comprised of five rings.

The planar structure was assembled through interpretation of the 2D NMR data (Table 1, Table S1 and Fig. 2). Briefly, a series of HMCBs from the two singlet aromatic protons H-11 and H-18 (δ_H 8.66 and 7.88, respectively) established a substituted benzene ring (C-10-12 and C-17-19; D-ring). HMCBs from H-11 to C-13 extended the chromophore and provided an anchor point for the assembly of the E-ring. A suite of HMCBs to C-13 from H-14 and H-15 and COSY correlations from the latter to H-16 appended a substituted propenol chain to the carbonyl. An HMBC to the corresponding carbinol carbon C-16 from H-18 established the dihydro-hydroxynaphthalenone system. The remaining tricyclic system was constructed beginning with HMCBs from the angular methyl group H₃-20 to C-19 of dihydro-hydroxynaphthalenone system and to C-5, C-6,



Xestosaprol D (**1**) R₁ = OH R₂ = H R₃R₄ = O
Xestosaprol E (**2**) R₁R₂ = O R₃ = OH R₄ = H

Figure 1. Structures of Xestosaprol D (**1**) and E (**2**).

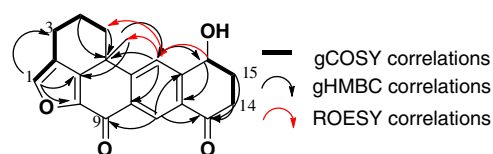


Figure 2. Key spectroscopic correlations of **1**.

* Corresponding author. Tel.: +1 808 956 5720; fax: +1 808 956 5908.
E-mail address: philipwi@hawaii.edu (P. Williams).

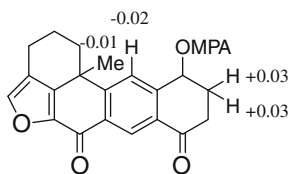
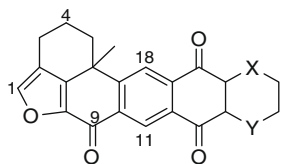


Figure 3. $\Delta\delta^{T1T2}$ values for (*R*)-MPA derivative of **1**.



Adociaquinone A (**3**) X = SO₂ Y = NH
Adociaquinone B (**4**) X = NH Y = SO₂

Figure 4. Active known metabolites isolated.

and C-7. Beginning with the geminal proton H₂-5, a series of correlations expanded this fragment into a six-membered ring including C-6 and C-7. HMBCs from the aromatic singlet H-1 to C-2, C-3 of this cyclohexenyl system suggested the final structure as depicted, although no direct evidence of the C-8/C-9 bond was available from the spectroscopic data. It should be noted that the structure of **1** hinges on the correct assignment of the H-11 to C-9/C-13 cross-peaks as 3-bond and H-18 to C-9/C-13 crosspeaks as 4-bond correlations. Evidences in support of these conclusions were the ROESY correlations between H-18 and H-5, H₃-20 and H-16, which were only possible in the constitutional isomer depicted.

We attempted to determine the absolute configuration of **1** via several different methods. Attempts to crystallize **1** from methanol, as previously reported for related compounds,² failed to provide crystals of sufficient quality for X-ray analysis. The use of alternative solvents yielded similar results. The absolute stereochemistry

of the C-16 chiral center was therefore established through variable temperature analysis of the (*R*)-(α -methoxyphenyl)acetic acid derivative. In 2004, Seco and co-workers established that the ¹H NMR spectra of a single MPA derivative taken at two different temperatures were a sufficient surrogate for the classical Mosher method involving two MTPA derivatives. In accord with their report,⁹ the calculated $\Delta\delta^{T1T2}$ values (Fig. 3) indicate a *R*-configuration at C-16. Unfortunately, no clear NOE correlation was observed between H-16 and the methyl H-20 which would have allowed the configuration at these centers to be related. Attempts, via NOE and ROE experiments, to relate the MPA moiety to the C-20 methyl in order to deduce the configuration at the latter center proved unsuccessful as well, due to the hydrolysis of the MPA ester. In a final attempt to deduce the configuration of C-6, we sought to convert **1** to a derivative for which its circular dichroism spectrum could be correlated to an intermediate (compound **8** in reference¹⁰) prepared by Harada in his classical twisted-diene CD analysis of halenaquinol.¹⁰ While oxidation of **1** to the *p*-naphthalenediol proceeded smoothly under classical Jones conditions, methylation of this derivative using iodomethane and K₂CO₃, as described by Harada, resulted in a complex mixture from which none of the desired product could be identified by LC-MS or ¹H NMR analysis. Thus, the absolute configuration of C-6 remains unassigned.

Further analysis of fractions generated during the isolation yielded Xestosaprol E (**2**). The spectral data of this optically active solid [α]_D -2.4 (c 0.1, MeOH) were nearly identical to **1**. Compound **2** was determined to be a constitutional isomer of **1** by mass spectrometry (C₂₀H₁₈O₄), but the UV maxima showed a slight bathochromic shift (λ_{max} 270 and 319 nm) indicating that the chromophore was modified. Analysis of the 2D data (Table S2) established that the positions of carbonyl and hydroxyl groups in the E-ring were reversed. The signal for H-11 was shifted to a higher field (**2** δ_H 8.45; **1** δ_H 8.66) and H-18 was shifted to a lower field (**2** δ_H 8.12; **1** δ_H 7.88). The latter proton showed a strong HMBC to the carbonyl signal at δ_C 198.8 (C-16), which provided the key data needed to establish the planar structure of **2**.

Compounds **1** and **2** were accompanied by the structurally related compounds, adociaquinones A (**3**)⁵ and B (**4**)⁵ along with

Table 1
NMR spectroscopic data (500 MHz) in CD₃CN for **1** and **2**

Position	1		2	
	δ_C , type ^a	δ_H (J in Hz)	δ_C , type ^a	δ_H (J in Hz)
1	145.8, CH	7.61, t (1.3)	146.0, CH	7.62, t (1.4)
2	122.8, qC		122.8, qC	
3	17.4, CH ₂	2.83, m	17.4, CH ₂	2.58, m
4	19.1, CH ₂	2.62, m	19.0, CH ₂	2.82, m
		2.25, m		2.07, m
5	31.9, CH ₂	2.10, m	31.9, CH ₂	2.25, m
		2.51, dt (12.8, 3.6)		2.54, m
6	37.9, qC	1.62, ddd (13.0, 12.9, 4.3)	37.4, qC	1.67, ddd (13.1, 12.8, 4.3)
7	148.2, qC		149.0, qC	
8	144.8, qC		145.0, qC	
9	172.2, qC		172.2, qC	
10	133.9, qC		138.3, qC	
11	126.7, CH	8.66, s	127.5, CH	8.45, s
12	130.7, qC		146.0, qC	
13	197.5, qC		67.5, CH	4.97, dd (8.7, 3.9)
14	36.3, CH ₂	2.82, dd (6.3, 4.4)	32.7, CH ₂	2.09, m
		2.64, m		2.34, m
15	32.7, CH ₂	2.35, m	36.3, CH ₂	2.84, m
		2.07, m		2.64, m
16	67.8, CH	4.98, dd (9.0, 4.1)	198.8, qC	
17	151.1, qC		134.4, qC	
18	125.2, CH	7.88, s	124.0, CH	8.12, s
19	157.1, qC		151.6, qC	
20	32.4, CH ₃	1.50, s	32.4, CH ₃	1.46, s

^a Type deduced by HSQC.

three additional members of the adociaquinone-xestoquinone family: Xestosaprol A,¹¹ 3,13-dideoxo-1,2, 13,15-tetrahydro-3-13-dihydroxyhalenaquinone,⁵ and 13,14,15,16-tetrahydroxestoquinol.⁵ These compounds were identified through comparison of their spectral data with previously published values (Fig. 4).

During preliminary screening, the ethyl acetate extract of this sponge displayed significant antimicrobial activity against multiple-resistant *Staphylococcus aureus* (ATCC 43300). Bioassay guided fractionation attributed this effect to the cytotoxins adociaquinones A (**3**) and B (**4**), with IC₅₀ values of 9.47 and 4.23 µg/ml, respectively.¹² To the best of our knowledge, this activity has not been previously reported for **3** and **4**. Compound **4** has been shown to inhibit topoisomerase II in CHO cell line xrs-6, not by intercalation as might be expected, but possibly by freezing the enzyme-DNA cleavable complex.¹³ Based on our findings then, **3** and **4** could potentially inhibit either gyrase B or topoisomerase IV, the bacterial targets of the quinolone antibiotics. The latter is generally the target in gram-positive organisms.¹⁴

In comparison, compounds **1** and **2** did not display an appreciable antimicrobial (VRE, *E. coli*, MRSA, SA) or cytotoxic effect (SKOV-3 cells, IC₅₀ > 50 µg/mL) and did not significantly activate or inhibit the oncogene Protein Kinase C (PKCδ). These data suggest that the sulfone and/or the secondary amine are critical for the observed antimicrobial and cytotoxic activities. Pure Xestosaprol D (**1**) did weakly inhibit the aspartic protease BACE-1, believed to be a central enzyme in the etiology of Alzheimer's disease,¹⁵ with an IC₅₀ value of approximately 30 µg/mL. The predicted log P¹⁶ of 2.62 and the low molecular weight for Xestosaprol D are in the optimal range to allow sufficient penetration of the blood–brain barrier,¹⁷ often the major hurdles for CNS drug development. As such, **1** represents a new non-peptidic scaffold that may serve as a viable starting point for optimization of a new structural class of BACE1 inhibitors.

Acknowledgments

This work was funded by grants from the Victoria S. and Bradley L. Geist Foundation (20070461). Upgrades of the NMR instrumen-

tation were provided by the CRIF program of the NSF (CH E9974921) and the Elsa Pardee Foundation. The purchase of the Agilent LC-MS was funded by the DOD (W911NF-04-1-0344). We thank W. Yoshida for the NMR data, A. Sorribas for the BACE1 data, and R. Barlow for the cytotoxicity data.

Supplementary data

Supplementary data (experimental procedures, tabulated NMR data for **1** and **2**, and copies of the spectroscopic data for all new compounds) associated with this article can be found, in the online version, at doi:10.1016/j.tetlet.2009.11.132.

References and notes

1. De-Almeida Leone, P.; Carroll, A. R.; Towerzey, L.; King, G.; McArdle, B. M.; Kern, G.; Fisher, S.; Hopper, J. N. A.; Quinn, R. J. *Org. Lett.* **2008**, *10*, 2585.
2. Roll, D. M.; Scheuer, P. J.; Matsumoto, G. K.; Clardy, J. *J. Am. Chem. Soc.* **1983**, *105*, 6177.
3. Nakamura, M.; Kakuda, T.; Qi, J.; Hirata, M.; Shintani, T.; Yoshioka, Y.; Okamoto, T.; Oba, Y.; Nakamura, H.; Ojika, M. *Biosci., Biotechnol., Biochem.* **2005**, *69*, 1749.
4. Nakamura, H.; Kobayashi, J.; Kobayashi, M.; Ohizumi, Y.; Hirata, Y. *Chem. Lett.* **1985**, *14*, 713.
5. Schmitz, F. J.; Bloor, S. J. *J. Org. Chem.* **1988**, *53*, 3922.
6. Lee, R. H.; Slate, D. L.; Moretti, R.; Alvi, K. A.; Crews, P. *Biochem. Biophys. Res. Commun.* **1992**, *184*, 765.
7. Bae, M.; Tsuji, T.; Kondo, K.; Hirase, T.; Ishibashi, M.; Shigemori, H.; Kobayashi, J. *Biosci., Biotechnol., Biochem.* **1993**, *57*, 330.
8. Nakamura, M.; Kakuda, T.; Oba, Y.; Ojika, M.; Nakamura, H. *Bioorg. Med. Chem.* **2003**, *11*, 3077.
9. Seco, J. M.; Quiñoá, E.; Riguera, R. *Chem. Rev.* **2004**, *104*, 17.
10. Harada, N.; Uda, H.; Kobayashi, M.; Shimizu, N.; Kitagawa, I. *J. Am. Chem. Soc.* **1989**, *111*, 5668.
11. Kobayashi, J.; Hirase, T.; Shigemori, H.; Ishibashi, M.; Tsuji, T.; Sasaki, T. *J. Nat. Prod.* **1992**, *55*, 994.
12. It should be noted that the crude extract displayed no antibiotic effect against *E. coli*, *S. aureus*, or VRE at the highest concentration tested.
13. Concepción, G. C.; Foderaro, T. A.; Eldredge, G. S.; Lobkovsky, E.; Clardy, J.; Barrows, L. R.; Ireland, C. M. *J. Med. Chem.* **1995**, *38*, 4503.
14. Hooper, D. In *Principles and Practices of Infectious Diseases*; Mandell, G. L., Bennertt, J. E., Dolin, R., Mandell, D., Eds.; Churchill Livingstone: Philadelphia, 2000; pp 404–423.
15. Hardy, J. *Curr. Alzheimer Res.* **2006**, *3*, 71.
16. Log P predicted using ACD version 12.0.
17. Hansch, C.; Björkroth, J. P.; Leo, A. *J. Pharm. Sci.* **1987**, *76*, 663.